A novel registration-based approach for 3D assessment of posttraumatic distal humeral deformities

Vlachopoulos, Lazaros ; Carrillo, Fabio ; Gerber, Christian ; Székely, Gábor ; Fürnstahl, Philipp

Abstract: BACKGROUND: With current 3-dimensional (3D) computer-based methods for the assessment of deformities, a surface registration method is applied to superimpose a computer model of the pathological bone onto a mirrored computer model of the contralateral side. However, because of bilateral differences, especially in humeral torsion, such template-based approaches may introduce bias in the assessment of a distal humeral deformity. We hypothesized that a novel registration approach might prove superior to the current approach in reducing such bias, thus yielding improved accuracy of 3D assessment of distal humeral deformities. METHODS: Three-dimensional triangular surface models were generated from computed tomographic (CT) data of 100 paired humeri without a pathological condition. Humeral segments of varying, predetermined lengths, excluding the distal part of the humerus, were defined. A surface registration algorithm was applied to superimpose the humeral models of both sides based on each selected segment. Humeral contralateral registration (HCR) errors, defined as the residual differences in apparent 3D orientation between the distal parts, were evaluated. RESULTS: The mean HCR error (and standard deviation) using the distal-most humeral shaft segment to assess the angular orientation was 2.3° ± 1.1 (range, 0.5° to 5.8°). Including the humeral head in the surface registration algorithm, however, as is done currently, resulted in a higher HCR error ($p < 0.001$). The HCR error using the proximal-most segment was >10° in 20% of the cases and between 5° and 10° in an additional 50% of the cases. By comparison, using the proposed distal-most humeral shaft segment, the HCR error was between 5° and 10° in only 2% of cases, and was never >10°. The proximal segments are nevertheless used in the proposed method for registering humeral length. CONCLUSIONS: The proposed new approach yields a deformity assessment that is less prone to bias arising from inherent bilateral differences and therefore is more accurate than current surface registration approaches. CLINICAL RELEVANCE: Accurate 3D assessment is of fundamental importance if computer-based methods are applied in the correction of posttraumatic deformities.

DOI: https://doi.org/10.2106/JBJS.16.01166

A Novel Registration-Based Approach for 3D Assessment of Posttraumatic Distal Humeral Deformities

Lazaros Vlachopoulos, MD, PhD, Fabio Carrillo, MSc, Christian Gerber, MD, FRCSEd(Hon), Gábor Székely, PhD, and Philipp Fürnstahl, PhD

Investigation performed at Balgrist University Hospital, Zurich, Switzerland

Background: With current 3-dimensional (3D) computer-based methods for the assessment of deformities, a surface registration method is applied to superimpose a computer model of the pathological bone onto a mirrored computer model of the contralateral side. However, because of bilateral differences, especially in humeral torsion, such template-based approaches may introduce bias in the assessment of a distal humeral deformity. We hypothesized that a novel registration approach might prove superior to the current approach in reducing such bias, thus yielding improved accuracy of 3D assessment of distal humeral deformities.

Methods: Three-dimensional triangular surface models were generated from computed tomographic (CT) data of 100 paired humeri without a pathological condition. Humeral segments of varying, predetermined lengths, excluding the distal part of the humerus, were defined. A surface registration algorithm was applied to superimpose the humeral models of both sides based on each selected segment. Humeral contralateral registration (HCR) errors, defined as the residual differences in apparent 3D orientation between the distal parts, were evaluated.

Results: The mean HCR error (and standard deviation) using the distal-most humeral shaft segment to assess the angular orientation was 2.3° ± 1.1 (range, 0.5° to 5.8°). Including the humeral head in the surface registration algorithm, however, as is done currently, resulted in a higher HCR error ($p < 0.001$). The HCR error using the proximal-most segment was >10° in 20% of the cases and between 5° and 10° in an additional 50% of the cases. By comparison, using the proposed distal-most humeral shaft segment, the HCR error was between 5° and 10° in only 2% of cases, and was never >10°. The proximal segments are nevertheless used in the proposed method for registering humeral length.

Conclusions: The proposed new approach yields a deformity assessment that is less prone to bias arising from inherent bilateral differences and therefore is more accurate than current surface registration approaches.

Clinical Relevance: Accurate 3D assessment is of fundamental importance if computer-based methods are applied in the correction of posttraumatic deformities.

Three-dimensional (3D) computer-based imaging methods have gained increasing importance in the surgical treatment of distal humeral deformities[1-5]. A recent study[4] demonstrated that corrective osteotomies of the distal aspect of the humerus can be performed precisely using preoperative 3D computer simulation along with patient-specific surgical guides at surgery. The main advantage of the preoperative simulation is the potential to assess the deformity in 3 dimensions, permitting the assessment of even small deviations from the normal anatomy in all anatomical planes. For example, a cubitus varus deformity resulting from a supracondylar fracture frequently has an accompanying extensional and/or rotational component[2].

The current state-of-the-art method in 3D deformity assessment relies on comparison of the pathological bone with a reconstruction template representing the normal anatomy. Currently, the contralateral anatomy most commonly serves as the basis of such reconstruction templates[1,4-8] because most

Disclosure: This work was funded, in part, by the Swiss Canton of Zurich through a Highly Specialized Medicine (HSM2) grant. Additional funding was provided by the Balgrist Foundation and by the Promedica Foundation Switzerland. P.F. is a shareholder of Balgrist CARD (Computer Assisted Research and Development), a company developing preoperative planning software. The **Disclosure of Potential Conflicts of Interest** forms are provided with the online version of the article (http://links.lww.com/JBJS/E509).

geometric measurements are similar between both sides of an individual[7-9]. A surface registration method is applied to superimpose the model of the pathological side onto the mirrored model of the contralateral side[1,3,5,10]. In previous studies[1,3,10], the whole proximal segment of the humerus (i.e., the humeral head, greater tuberosity, and shaft) was included when superimposing such models. However, and especially if there are underlying side-to-side differences in the twist about the humeral axis (humeral torsion) in a given individual[8,9], a superimposition involving the entire proximal segment of the humerus[1,3,10] might introduce considerable error in determining distal humeral deformity.

In the present study, we systematically selected different segments of the humerus for inclusion in the superimposition, and we evaluated the effect of these different segmental inclusions on the robustness against bias due to underlying bilateral differences. On the basis of those results, we identified a new segment-selection strategy that may better compensate for underlying bilateral differences than does the current approach, thus providing better 3D assessment of distal humeral deformities.

Material and Methods

The Swiss Institute for Computer Assisted Surgery (SICAS) provided full-body computed tomography (CT) data for 50 cadavers (including the entire humerus on both sides). The in-plane (x-y) resolution of the CT scans ranged from pixel sizes of 0.9 × 0.9 mm to 1.27 × 1.27 mm. The slice thickness varied from 0.5 mm to 0.6 mm. The average donor age (and standard deviation) was 52.1 ± 20.0 years (range, 19 to 90 years). There were 32 male and 18 female donors. The average height was 172.4 ± 8.7 cm (range, 154 to 187 cm), and the average weight was 68.4 ± 16.9 kg (range, 37 to 108 kg). Exclusion criteria were the presence of osteoarthritis or history of trauma. The specimens had been used previously for the development of computer algorithms for the measurement of the humeral anatomy in 3 dimensions[8]. Segmentation of the humerus was performed fully automatically using a previously described method[11]. A marching cubes algorithm[12] was applied to generate bilateral, 3D triangular surface models. Thereby, we obtained a manifold mesh only of the outer cortical layer. Subsequently, the models were imported into the planning software CASPA (Computer Assisted Surgery Planning Application) that was developed in-house (Balgrist CARD [Computer Assisted Research and Development]).

In the following section, before providing a detailed description of the proposed approach, we describe the current state-of-the-art method in 3D deformity assessment of malunited distal humeral fractures[1,3,5,10]. To analyze the robustness of the proposed approach against underlying bilateral humeral differences for an individual, we validated the method using bilateral humeral models showing no signs of a previous trauma or osteoarthritis.

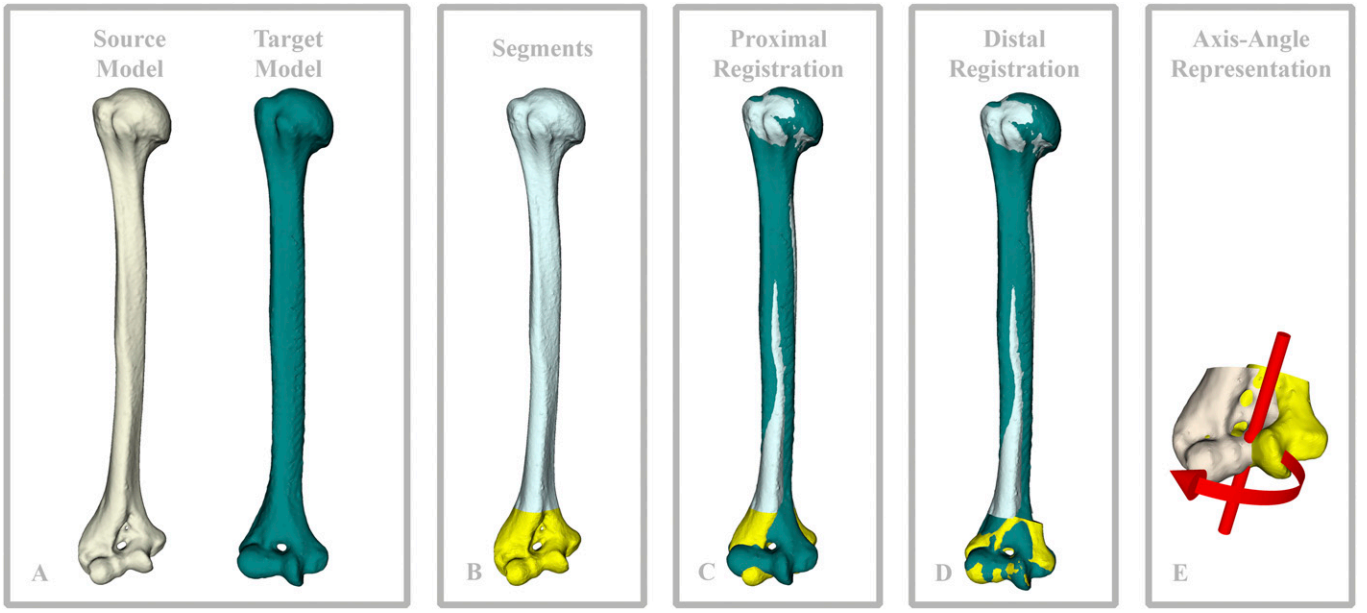

Fig. 1

Figs. 1-A through 1-E Template-based assessment of a distal humeral deformity. **Fig. 1-A** The mirrored left humerus (target model) serves as a reconstruction template for the assessment of the deformity of the right humerus (source model). **Fig. 1-B** One segment proximal to the assumed deformity (i.e., the blue segment, 85% of the length of the right humerus) and 1 segment distal to the assumed deformity (i.e., the yellow segment, 15% of the length of the humerus) are selected to quantify the deformity. **Figs. 1-C and 1-D** The proximal segment **(Fig. 1-C)** and the distal (elbow) segment **(Fig. 1-D)** are subsequently registered onto the mirrored left humerus using the ICP (iterative closest point) algorithm. **Fig. 1-E** The rotational difference of the elbow segment between the proximal registration and the distal registration is expressed in axis-angle representation, i.e., a rotation by a 3D angle of 35° (red arrow) about a calculated axis.

Current State-of-the-Art Deformity Assessment

The template-based approach is the most commonly used method for the 3D assessment of posttraumatic deformities[1,3,5,10]. With this approach, the mirrored contralateral humeral model serves as a reconstruction template (Fig. 1-A). To quantify a distal humeral deformity, 2 segments must be selected: a segment proximal to the pathological area, and a segment distal to the pathological area (Fig. 1-B). The proximal segment is selected in such a manner that it contains the humeral head, the greater tuberosity, and part of the shaft[3,10]. The distal (elbow) segment contains the medial and lateral epicondyles and the distal articular surface[3,10]. A surface registration method, such as the iterative closest point (ICP) algorithm[13,14], is applied to superimpose the bone models. First, the whole pathological bone model is superimposed on the whole reconstruction template with the proximal segment serving as the basis of registration (Fig. 1-C). Importantly, in this step, the distal segment of the pathological bone is superimposed on the distal segment of the reconstruction template solely on the basis of the ICP registration of the corresponding proximal segment. Finally, the distal segment of the pathological bone is registered on the distal segment of the reconstruction template, again using the ICP algorithm (Fig. 1-D). The relative 3D rotation and 3D translation of the distal segment in this final step quantify the malalignment. The rotational component of this malalignment is expressed in axis-angle representation (Fig. 1-E), i.e., as a rotation by a 3D angle about a calculated axis.

Effect of Segment Selection on Deformity Assessment

The principle of the ICP algorithm is to register a source model with a superimposed target model in such a way that the sum of the distances between all corresponding pairs of points on a given segment of interest of the surfaces of the 2 respective models is either 0 (identical model surfaces) or minimal (non-identical model surfaces).

In Figure 2, using a simplified representation, we schematically illustrate the effect on the deformity assessment when bilateral differences in humeral torsion are present without an additional pathological condition. The

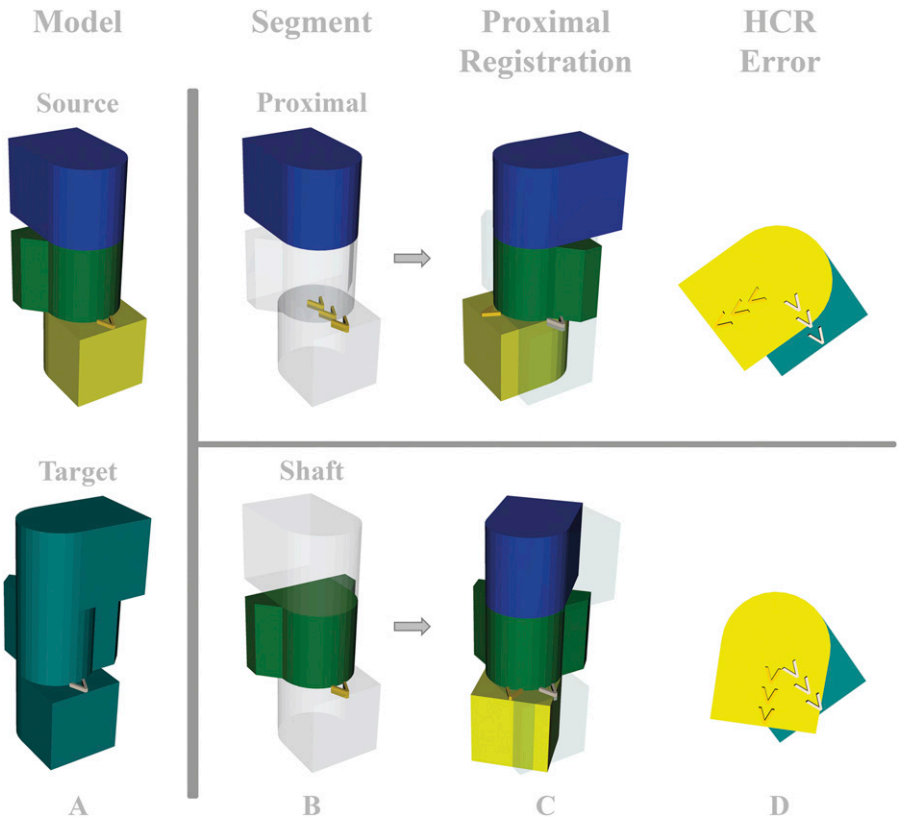

Fig. 2

Figs. 2-A through 2-D Schematic illustration of the effect of segment selection on the registration result. **Fig. 2-A** The source model represents a humeral model with a higher axial twist between proximal and distal parts compared with the target model. A cuboid represents the humeral head, a trapezoidal-shaped prism represents the humeral shaft, and a cube symbolizes the distal joint with the epicondyles. **Fig. 2-B** The selected segments used for the proximal registration are illustrated. In the upper panel, the segment used for proximal registration contains the humeral head, whereas in the lower panel, the shaft segment is instead used for proximal registration. **Fig. 2-C** Registration minimizes the difference between the surfaces of the selected segments. **Fig. 2-D** The segment selection influences the HCR (humeral contralateral registration) error.

simplified humeral representation consists of 3 prisms, aligned axially along a cylinder. A cuboid (blue) represents the humeral head, a trapezoidal-shaped prism (green) represents the humeral shaft, and a cube (yellow) symbolizes the "elbow" segment that includes the epicondyles. The difference in humeral torsion between the respective models is illustrated by the different rotation of the prisms around the cylinder (Fig. 2-A). In the example of Figure 2, the current state-of-the-art strategy[3,10] is denoted by the registration of the selected proximal segment (Fig. 2-B; upper panel). A different approach would be to select only parts of the shaft (Fig. 2-B; lower panel). The result of the ICP registration for these respective registration strategies is illustrated in Figure 2-C. In the first case (Fig. 2-C; upper panel), ICP registration minimizes the average distances between the surfaces of the proximal segments of the source and target models. This yields a precise registration of the proximal segment of the humerus. However, the apparent axial twist of the elbow segment is greater compared with that when registration is instead done using the shaft segment (Fig. 2-C; lower panel). We describe the residual difference in apparent 3D orientation between the distal parts of both humeri as the *humeral contralateral registration (HCR) error.* The HCR corresponds to the 3D angle in axis-angle representation when bilateral models without a pathological condition are analyzed. The influence of the segment selection on the HCR error is illustrated in Figure 2-D.

Novel Automatic Segment-Selection Approach

The previous description with our simplified illustration conceptually demonstrates how the current state-of-the-art method introduces bias when there are underlying differences bilaterally in humeral torsion. Applying this same concept to actual complex humeral anatomy, to quantify how using different humeral segments for registration may result in a smaller HCR error, we performed ICP registration experiments for each subject by processing the data in an automatic and standardized fashion. We defined the right humerus of a subject as the source model. The mirrored left contralateral humerus served as the target model. To demonstrate that the evaluation was not biased by the selection of the source versus target models, we repeated all computational experiments using the left humerus as the source model and the mirrored right humerus as the target model. This allowed assessment of the consistency of the method using the interclass correlation coefficient (ICC).

Registration experiments for the new approach were performed using the same general steps as described above for the current method of deformity assessment, except that several alternative segments were utilized for the proximal registration. For the distal registration that was used to quantify the HCR error, the same distal segment was used in all instances. The humeral segments were created by automatically dividing each source model on the basis of predetermined percentages of humeral length (Fig. 3-A). The 5 alternative proximal segments that included at least the humeral head and the greater tuberosity

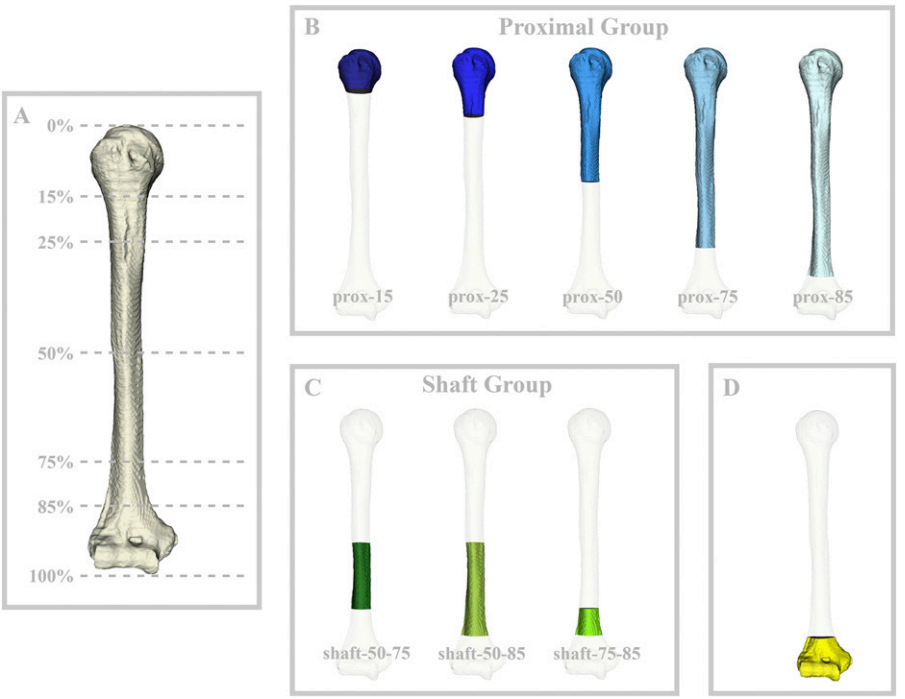

Fig. 3

Figs. 3-A through 3-D Generation of the segments defined for registration. **Fig. 3-A** Right humeral model, with humeral length expressed as a percentage, from the proximal end (0%) to the distal end (100%). **Figs. 3-B, 3-C, and 3-D** The defined segments for the proximal registration, including the proximal group **(Fig. 3-B)** and shaft group **(Fig 3-C)**, and for the distal registration to evaluate the HCR (humeral contralateral registration) error **(Fig. 3-D)**.

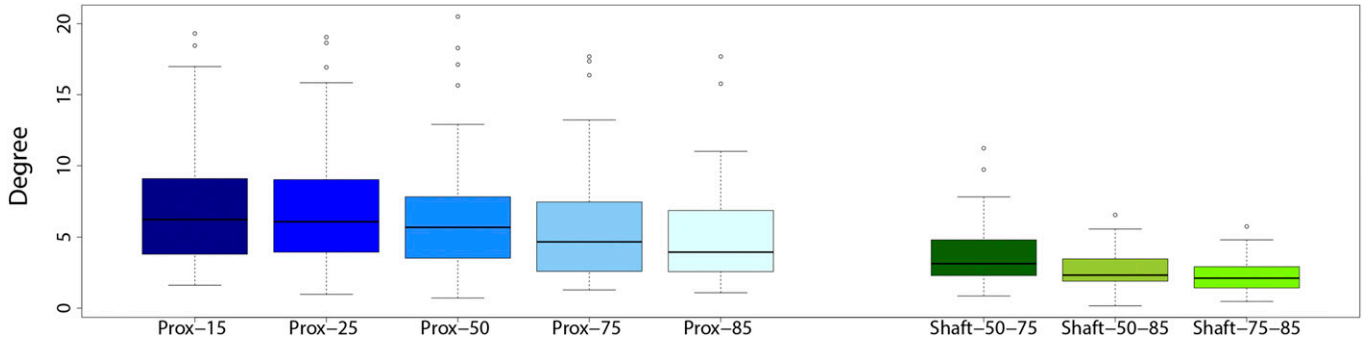

Fig. 4

Box plots of the HCR (humeral contralateral registration) error as a function of the selected segments. The end of each whisker indicates 1.5 times the interquartile range (IQR) between the lower and upper quartiles. The circles indicate outliers.

(*prox-15, prox-25, prox-50, prox-75,* and *prox-85,* i.e., those segments consistent with what would be used in the current state-of-the-art method[3,10]) were assigned to what was designated as the proximal group (Fig. 3-B). The remaining 3 alternative proximal segments (*shaft-50-75, shaft-50-85,* and *shaft-75-85*) were assigned to what was designated as the shaft group (Fig. 3-C).

The proximal registration reveals the deviation of the elbow segment between both anatomical humeri, analogous with the illustration in Figure 2. We determined the HCR error by then registering the elbow segment (distal registration, Fig. 1-D). For this HCR calculation, we consistently used a distal segment that included the medial and lateral epicondyles and the distal articular surface[3,10], in all instances, involving 15% of the total length of the humerus (elbow segment, Fig. 3-D). Again, the HCR error for 2 identically oriented elbow segments with identical anatomy would be 0. Note that we consistently use the same color coding to represent the defined segments.

Statistical Analysis

A Mauchly sphericity test revealed a violation of the assumption of sphericity. Therefore, we applied the nonparametric Friedman rank-sum test, with the segment as a group factor and the individuals as a block factor for the analysis of the HCR error as a function of the selected segment. Post-hoc analysis was performed using the Wilcoxon signed-rank test with Bonferroni adjustment. The significance level was set at $p < 0.05$. The consistency of the method was assessed with the ICC (2-way random-effects model). For graphical visualization, Tukey box plots were used, with the end of each whisker indicating 1.5 times the interquartile range (IQR) between the lower and upper quartiles and the circles indicating the outliers. All reported HCR errors were calculated from the average of the absolute values, regardless of whether the right or the left humeri were selected as the source models.

Results

The Friedman rank-sum test revealed a significant effect of the selected segments on the HCR error (chi-square = 153; $p < 0.0001$). Figure 4 shows the HCR error for each segment of both the proximal and shaft groups. Twenty-eight paired Wilcoxon signed-rank tests were performed for post-hoc analysis. The Bonferroni-adjusted p value was $0.05/28 \approx$

TABLE I HCR Error of the Distal Segment of the Humerus for Each Selected Proximal Segment, with Corresponding ICC*

	HCR Error (°)				
Selected Segment	Mean	Std. Dev.	Median	Range	ICC (95% CI)
Prox-15	7.4	4.5	6.2	1.6-19.3	1.00 (0.99-1.00)
Prox-25	7.2	4.5	6.1	1.0-19.1	1.00 (0.99-1.00)
Prox-50	6.7	4.5	5.7	0.7-20.5	1.00 (0.99-1.00)
Prox-75	5.7	4.3	4.7	1.3-17.7	1.00 (0.99-1.00)
Prox-85	5.2	3.7	4.0	1.1-17.7	0.98 (0.97-1.00)
Shaft-50-75	3.8	2.3	3.1	0.9-11.2	0.94 (0.89-0.96)
Shaft-50-85	2.6	1.3	2.3	0.2-6.6	0.94 (0.90-0.97)
Shaft-75-85	2.3	1.1	2.1	0.5-5.8	0.93 (0.88-0.96)

*HCR = humeral contralateral registration, ICC = interclass correlation coefficient, and CI = confidence interval.

0.002 for each individual comparison in order to retain the prescribed family-wise error rate of 0.05. The ICC was ≥0.93 for all selected segments (Table I). For each humeral pair, we performed 8 left-to-right and 8 right-to-left registrations, which yielded 800 registration experiments in total.

The HCR errors for the shaft-50-85 and shaft-75-85 segments were significantly smaller than the HCR errors for the 5 segments of the proximal group ($p < 0.001$) and for the shaft-50-75 segment ($p < 0.001$). We did not find a significant difference in HCR error between the shaft-75-85 and shaft-50-85 segments ($p = 0.01$). The HCR error for the shaft-50-75 segment was significantly smaller than the HCR errors for the prox-15, prox-25, and prox-50 segments ($p < 0.001$). We did not find a significant difference in HCR error between the shaft-50-75 segment and the prox-75 segment ($p = 0.004$) or between the shaft-50-75 segment and the prox-85 segment ($p = 0.02$). We also did not find a significant difference in HCR error between the prox-15 and prox-25 segments ($p = 0.01$). All other differences in the HCR errors between segments within the proximal group were significant ($p < 0.001$).

The HCR error for the prox-15 segment was >10° in 20% of the cases, and it was between 5° and 10° in an additional 50% of the cases. The HCR error for the shaft-75-85 segment was between 5° and 10° in 2% of the cases, and it was never >10°. Table I shows the mean, standard deviation, and range of the HCR errors for all segments.

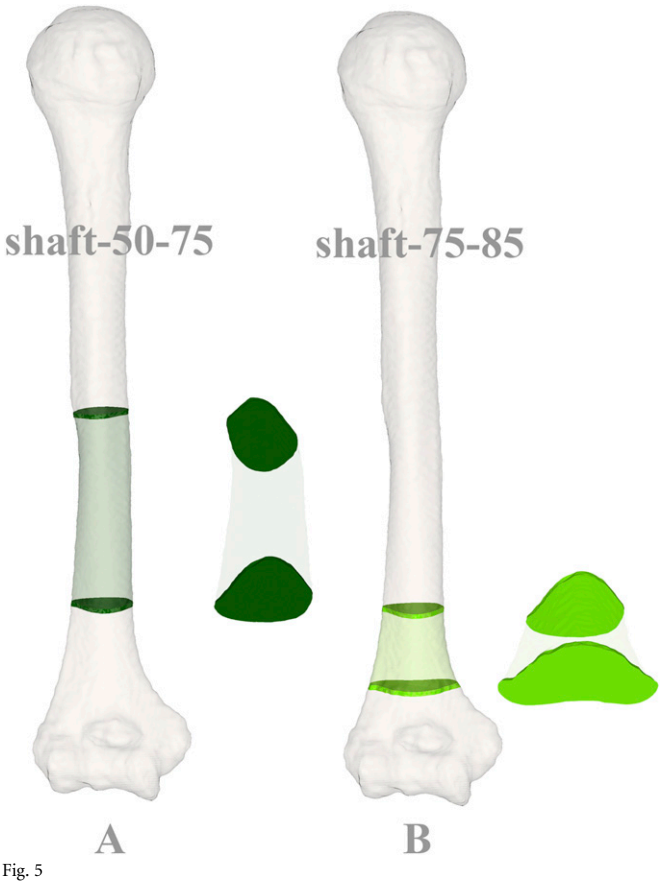

Fig. 5

Idiosyncratic features of the distal aspect of the humerus. Anterior and cross-sectional views of the shaft-50-75 segment **(Fig. 5-A)** and the shaft-75-85 segment **(Fig. 5-B)** are illustrated.

Discussion

The benefits of 3D computer-assisted corrective osteotomies of distal humeral deformities have already been emphasized[4,5]. In this context, the 3D assessment of distal humeral deformities[1,3-5,10,15] has gained importance, as has the development of a surgical technique to perform the surgery as planned on the computer[1,3-5,10,15]. The reliability of the contralateral humerus as a reconstruction template is of fundamental importance to restore the pretraumatic anatomy as precisely as possible, as the reconstruction template influences all subsequent steps of the procedure[5]. In other words, a high HCR error would tend to result in an inaccurate restoration of the pretraumatic anatomy.

We investigated the effect of various selected segments on the 3D registration-based deformity assessment. Authors of previous studies have proposed using the entire nonpathological proximal segment for the proximal registration[3,10]. However, the farther away that proximal humeral regions used for the proximal registration lie from the distal area of interest, the greater the tendency for error propagation. Takeyasu et al.[2] reported that most patients with a posttraumatic cubitus varus deformity have an accompanying extension and/or rotational deformity of ≥10°, highlighting the 3D nature of these deformities. Nevertheless, the results of deformity assessment by Takeyasu et al. should be interpreted with caution, since segments similar to those of the proximal group in the present study were used for registration with the reconstruction template[3].

Both in a cadaveric study[15] and in vivo[4], Omori et al. demonstrated that the 3D preoperative plan can be realized very accurately during surgery with patient-specific guides. Those authors reported a mean error of 0.6° ± 0.7° in varus-valgus orientation and 0.8° ± 1.3° in flexion-extension orientation. The error in axial rotation was higher (mean, 2.9° ± 2.8°), with a maximum error of 9.4°. The postoperative evaluation was performed with what probably is the most precise current state-of-the-art technique. Although the results reported by Omori et al. are promising, their postoperative evaluation of accuracy represented only the difference between the performed correction and the preoperative plan, which does not necessarily correspond to the deviation from the pretraumatic condition.

Another approach to achieving correspondence between CT-based preoperatively created surface models and the intraoperative situation was analyzed by McDonald et al.[16]. By simulating different situations of articular bone loss, those authors demonstrated that close alignment of a preoperative image with intraoperative surface data can be achieved (rotational error, 0.4° ± 0.1°) if the distal humeral shaft were scanned by the surgeon using a laser scanner. It should be noted that, again, this rotational error captured only the implementation of the preoperative plan.

McDonald et al.[7] also demonstrated that anthropometric distal humeral measurements (i.e., the flexion-extension axis of the elbow and the offset) are similar for paired specimens. Registration of the elbow segment, such as that defined in the present study, to the healthy contralateral anatomy yielded a side-to-side difference of approximately 1.0° and 0.5 mm. Furthermore, registration of the elbow segment was possible even in the presence of severe bone loss at the articular surface and did not affect the flexion-extension axis of the elbow or the offset. These findings[7,16] reinforce the results of the present study. However, in the work by McDonald et al., the size of the distal humeral shaft segment used for the registration was not defined[7,16]. In addition, the segments selected for registration seemed to correspond only to the elbow segment as defined in the present study. Thereby, only the accuracy of the distal registration of the deformity assessment was analyzed.

In the present study, the method for the accurate approximation of the pretraumatic distal humeral anatomy is described only in the context of corrective osteotomies of the distal aspect of the humerus. The main reason for this is that 3D preoperative planning and the use of patient-specific guides are well accepted for such procedures. Thus, it was possible to directly demonstrate the benefit of this new approach as compared with the present state-of-the-art method. By implication, however, this new method is probably also applicable to other procedures that rely on an accurate approximation of the pretraumatic distal humeral anatomy (e.g., navigation for total elbow arthroplasty[17]).

Compared with the current state-of-the-art method[1,3,10], the present results demonstrate that the HCR error is less sensitive to intra-individual differences if only segments of the distal humeral shaft (shaft-50-85 or shaft-75-85) are selected for registration. We analyzed the influence of the distance from the area of interest to the segment selected for registration, but it needs to be borne in mind that differences in bone shape play a role as well. Figure 5 illustrates the cross-sectional shape of the shaft-50-75 and shaft-75-85 segments. The presence of idiosyncratic features is obviously relevant for registration-based approaches that compensate for bilateral differences (such as differences in axial twist). For that reason, the magnitude of HCR error and the consistency of registration would need to be validated separately when considering implementing this new approach for other skeletal sites, as the idiosyncratic features that are involved would be different.

One limitation of the present study was that, similar to the state-of-the-art method, the preoperative assessment of the deformity can be applied only if the contralateral bone is normal (without deformity). It is crucial that the segment used for the proximal registration be proximal to the pathological area. However, since the most-proximal part of the humerus is not necessary for the registration, the present method can be used even in the presence of a pathological condition of the proximal humeral anatomy. Nevertheless, this novel approach yields a deformity assessment that is more robust against bilateral differences and more precise than the current state-of-the-art method for reconstruction of the pretraumatic angular orientation of the elbow. Furthermore, with this new approach, restoration of humeral length might be influenced by bilateral differences in the diameter of the humeral shaft. Therefore, we propose reconstructing the length so as to replicate the length of the contralateral humeral model, since the contralateral anatomy is assumed to be a reliable template for the humeral length[8]. In conclusion, our new approach strengthens the benefits of, and improves on, the application of the current technique for corrective distal humeral osteotomies. ■

Lazaros Vlachopoulos, MD, PhD[1,2]
Fabio Carrillo, MSc[1]
Christian Gerber, MD, FRCSEd(Hon)[1]
Gábor Székely, PhD[2]
Philipp Fürnstahl, PhD[1]

[1]Computer Assisted Research and Development Group (L.V., F.C., and P.F.) and Department of Orthopaedics (C.G.), Balgrist University Hospital, University of Zurich, Zurich, Switzerland

[2]Computer Vision Laboratory, ETH Zurich, Zurich, Switzerland

E-mail address for L. Vlachopoulos: lazaros.vlachopoulos@balgrist.ch

ORCID iD for L. Vlachopoulos: 0000-0001-8526-6032

References

1. Murase T, Oka K, Moritomo H, Goto A, Yoshikawa H, Sugamoto K. Three-dimensional corrective osteotomy of malunited fractures of the upper extremity with use of a computer simulation system. J Bone Joint Surg Am. 2008 Nov;90 (11):2375-89.

2. Takeyasu Y, Murase T, Miyake J, Oka K, Arimitsu S, Moritomo H, Sugamoto K, Yoshikawa H. Three-dimensional analysis of cubitus varus deformity after supracondylar fractures of the humerus. J Shoulder Elbow Surg. 2011 Apr;20 (3):440-8.

3. Takeyasu Y, Oka K, Miyake J, Kataoka T, Moritomo H, Murase T. Preoperative, computer simulation-based, three-dimensional corrective osteotomy for cubitus varus deformity with use of a custom-designed surgical device. J Bone Joint Surg Am. 2013 Nov 20;95(22):e173.

4. Omori S, Murase T, Oka K, Kawanishi Y, Oura K, Tanaka H, Yoshikawa H. Postoperative accuracy analysis of three-dimensional corrective osteotomy for cubitus varus deformity with a custom-made surgical guide based on computer simulation. J Shoulder Elbow Surg. 2015 Feb;24(2):242-9.

5. Vlachopoulos L, Schweizer A, Meyer DC, Gerber C, Fürnstahl P. Three-dimensional corrective osteotomies of complex malunited humeral fractures using patient-specific guides. J Shoulder Elbow Surg. 2016 Dec;25(12):2040-7. Epub 2016 Aug 5.

6. Bicknell RT, DeLude JA, Kedgley AE, Ferreira LM, Dunning CE, King GJ, Faber KJ, Johnson JA, Drosdowech DS. Early experience with computer-assisted shoulder hemiarthroplasty for fractures of the proximal humerus: development of a novel technique and an in vitro comparison with traditional methods. J Shoulder Elbow Surg. 2007 May-Jun;16(3)(Suppl):S117-25: 25. Epub 2007 Jan 17..

7. McDonald CP, Peters TM, King GJ, Johnson JA. Computer assisted surgery of the distal humerus can employ contralateral images for pre-operative planning, registration, and surgical intervention. J Shoulder Elbow Surg. 2009 May-Jun;18 (3):469-77.

8. Vlachopoulos L, Dünner C, Gass T, Graf M, Goksel O, Gerber C, Székely G, Fürnstahl P. Computer algorithms for three-dimensional measurement of humeral anatomy: analysis of 140 paired humeri. J Shoulder Elbow Surg. 2016 Feb;25(2): e38-48. Epub 2015 Oct 4.

9. DeLude JA, Bicknell RT, MacKenzie GA, Ferreira LM, Dunning CE, King GJ, Johnson JA, Drosdowech DS. An anthropometric study of the bilateral anatomy of the humerus. J Shoulder Elbow Surg. 2007 Jul-Aug;16(4):477-83. Epub 2007 Mar 23.

10. Murase T, Takeyasu Y, Oka K, Kataoka T, Tanaka H, Yoshikawa H. Three-dimensional corrective osteotomy for cubitus varus deformity with use of custom-made surgical guides. JBJS Essent Surg Tech. 2014;4(1):e6.

11. Gass T, Székely G, Goksel O. Simultaneous segmentation and multiresolution nonrigid atlas registration. IEEE Trans Image Process. 2014 Jul;23(7):2931-43. Epub 2014 May 7.

12. Lorensen WE, Cline HE. Marching cubes: a high resolution 3D surface construction algorithm. ACM Siggraph Computer Graphics Newsletter. 1987 Jul;21 (4):163-9

13. Audette MA, Ferrie FP, Peters TM. An algorithmic overview of surface registration techniques for medical imaging. Med Image Anal. 2000 Sep;4(3):201-17.

14. Chen Y, Medioni G. Object modeling by registration of multiple range images. Proceedings of the 1991 IEEE International Conference on Robotics and Automation; 1991; Sacramento, California.

15. Omori S, Murase T, Kataoka T, Kawanishi Y, Oura K, Miyake J, Tanaka H, Yoshikawa H. Three-dimensional corrective osteotomy using a patient-specific osteotomy guide and bone plate based on a computer simulation system: accuracy analysis in a cadaver study. Int J Med Robot. 2014 Jun;10(2):196-202. Epub 2013 Sep 18.

16. McDonald CP, Beaton BJ, King GJ, Peters TM, Johnson JA. The effect of anatomic landmark selection of the distal humerus on registration accuracy in computer-assisted elbow surgery. J Shoulder Elbow Surg. 2008 Sep-Oct;17 (5):833-43. Epub 2008 Jun 24.

17. McDonald CP, Johnson JA, Peters TM, King GJ. Image-based navigation improves the positioning of the humeral component in total elbow arthroplasty. J Shoulder Elbow Surg. 2010 Jun;19(4):533-43. Epub 2010 Feb 4.